Spectrally tailored mid-infrared super-continuum generation in a buried waveguide spanning 1750nm to 5000nm for atmospheric transmission

AIP | Applied Physics Letters

Spectrally tailored mid-infrared super-continuum generation in a buried waveguide spanning 1750nm to 5000nm for atmospheric transmission

J. McCarthy, H. Bookey, S. Beecher, R. Lamb, I. Elder, and A. K. Kar

Citation: Applied Physics Letters **103**, 151103 (2013); doi: 10.1063/1.4824358
View online: http://dx.doi.org/10.1063/1.4824358
View Table of Contents: http://scitation.aip.org/content/aip/journal/apl/103/15?ver=pdfcov
Published by the AIP Publishing

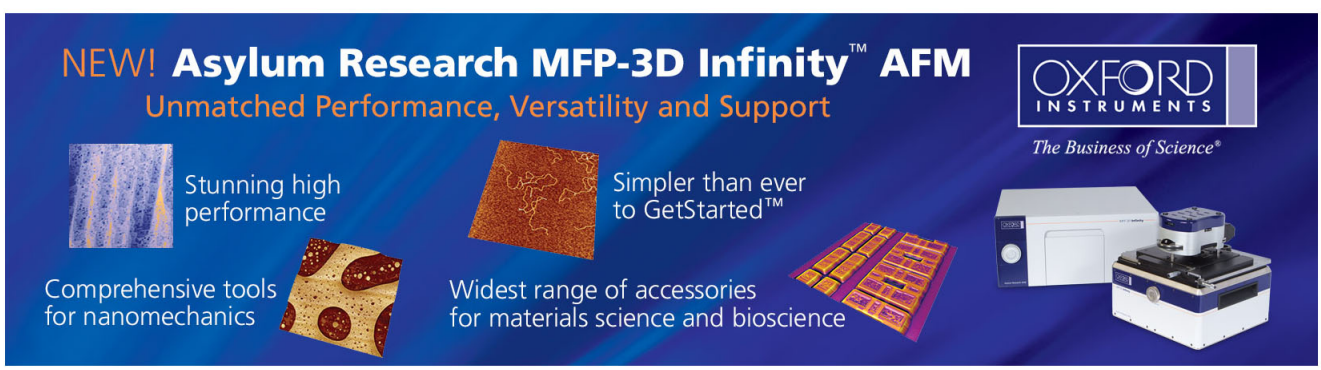

Spectrally tailored mid-infrared super-continuum generation in a buried waveguide spanning 1750 nm to 5000 nm for atmospheric transmission

J. McCarthy,[1] H. Bookey,[1,2] S. Beecher,[3] R. Lamb,[4] I. Elder,[4] and A. K. Kar[1]
[1]*Insitute of Photonics and Quantum Sciences, School of Engineering and Physical Sciences, Heriot Watt University, Edinburgh EH14 4AS, United Kingdom*
[2]*Fraunhofer Centre for Applied Photonics, 347 Cathedral St., University Centre, Glasgow G1 2TB, United Kingdom*
[3]*Optoelectronics Research Centre, University of Southampton, SO17 1BJ, United Kingdom*
[4]*SELEX ES, Crewe Toll, 2 Crewe Road, Edinburgh EH5 2XS, United Kingdom*

(Received 22 August 2013; accepted 12 September 2013; published online 7 October 2013)

We show how nonlinear spectral broadening in a buried chalcogenide mid-infrared waveguide can be used to reshape the spectrum of a femtosecond pulse train at 4260 nm in order to reduce the effects of atmospheric absorption due to carbon dioxide. The nonlinear spectral broadening results in the source with −20 dB spectral width spanning over 3500 nm, from 1700 nm to 5200 nm. This represents a potential route to tailored sources for long-range mid-infrared applications. © *2013 AIP Publishing LLC*. [http://dx.doi.org/10.1063/1.4824358]

The mid infrared atmospheric transmission window from 2 to 5 μm is of interest for biomedical,[1,2] directed infrared counter-measures,[3] and gas sensing applications[4,5] and consequently, there is motivation for the development of broadband sources in this region. Super-continuum (SC) generation in optical fibers and waveguides is a mature field and is well understood.[6,7] SC extending into the mid infrared spectral region is of interest for spectroscopy, nonlinear microscopy, optical metrology, optical coherence tomography, and frequency comb generation.

For efficient atmospheric transmission in the 3–5 μm window, it has previously been proposed to use the spectral shaping effects of self-phase modulation (SPM) to avoid the losses associated with carbon dioxide absorption at 4.25 μm.[8] Carbon dioxide absorption is the main contributor to transmission loss in the 2–5 μm window and by pumping a nonlinear material at a wavelength centered on a CO_2 absorption feature SPM can tailor the source spectrum such that the majority of the spectral energy density is distributed to other wavelengths within the transmission window. In this letter we present an experimental realization of this concept. Nonlinear spectral broadening of pulse trains having pump wavelengths beyond 4 μm has only been realized in bulk substrates[9] we present observations of supercontinuum generation in a guided wave device using a pump wavelength longer 4 microns.

SC sources are readily available and their long wavelength limits are often determined by the material linear transmission spectrum. Using chalcogenide glasses, it is possible to exploit excellent long wavelength transmission properties that are coupled with a high optical nonlinearity.[10] The progress in materials science over the last few years has meant that chalcogenide glasses of high optical quality are now commercially available and have been developed for fiber drawing applications.[11] There are several reports on the fabrication of non-silica fibers and fiber tapers for octave spanning SC extending into the mid infrared.[12–15] However, chalcogenide fibers are difficult to fabricate with low loss and are difficult to handle, although there is a recent report of a scheme to encase a chalcogenide nano-taper with a silica over-cladding.[16] For short pulse durations it is not necessary to have the long interaction lengths enabled by a fiber platform for optimum SC generation[17] and an optical chip would benefit integration with other components. Many of the techniques used to make integrated chalcogenide waveguides rely on multi-step deposition[18] or embossing[19] processes which have their own limitations. On the other hand, direct laser writing has been successfully utilized to fabricate buried singlemode waveguides in chalcogenides in a simple, repeatable, single step process.[20,21]

Buried waveguides were fabricated in the 9 mm long substrate using ultrafast laser inscription (ULI).[21] ULI is a convenient fabrication technique that offers three dimensional inscription capability: thus, it can be used in the fabrication of a number of complex optical devices.[22] Central to ULI is the nonlinear absorption of sub-bandgap radiation inside a substrate, it can therefore be used to fabricate structures in a wide range of different materials. Our previous work on ULI in chalcogenides was based on single-scan inscription,[20,21] where the waveguide cross-section exhibited a "teardrop" structure. Here we use a multi-scan inscription technique,[23] allowing greater control over the waveguide cross-section and energy deposition. In Fig. 1(b), the facet image of an inscribed waveguide and the corresponding mode profile at 4.26 μm is shown. The waveguide cross-section is very different to those previously reported in chalcogenide glasses, due to lower energies required for multi-scan inscription, with no photo-darkening or regions of reduced refractive index in the material. The guided mode, shown in Fig. 1(c), is more confined and exhibits greater circular symmetry than previously reported waveguides inscribed in gallium lanthanum sulphide (GLS).[21] The field of view for both the facet image and mode profile is 100 μm. The $1/e^2$ mode field diameter (MFD) was measured to be 45.5 μm in the axis orthogonal to the waveguide axis and inscription laser propagation direction and 44.6 μm in the axis parallel to the inscription laser propagation direction. The structures terminate approximately 55 μm from the end

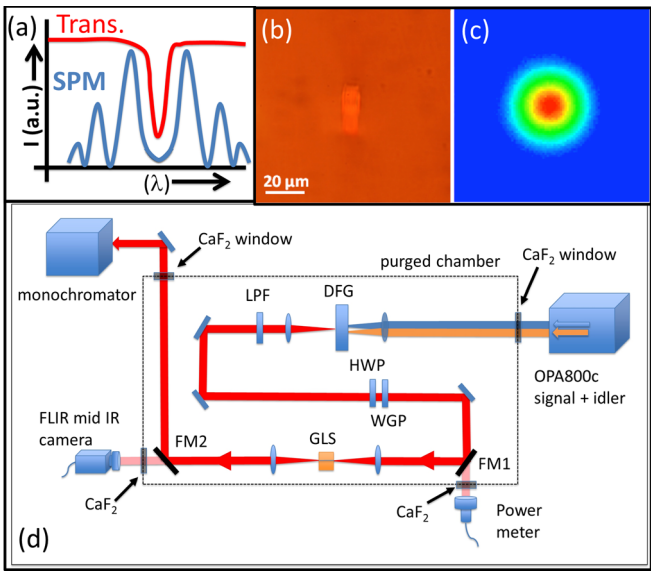

FIG. 1. The concept of using self-phase modulation to reshape a pulse spectrum (SPM) around an absorption feature (Trans.) is shown in (a). The GLS waveguide facet is shown in (b) and corresponding mode image (c) at 4260 nm on the same scale. (d) Experimental arrangement for the coupling of mid infrared pulse train into GLS waveguide. The signal and idler outputs from an OPA source are focused inside a difference frequency generation (DFG) crystal. LPF, long pass filter; HWP, half wave plate; WGP, wire grid polarizer; FM1 and FM2 are flip mirrors.

facets of the substrate and are observed to be single mode at 4.26 μm.

For continuum generation, the waveguide is pumped by a femtosecond optical parametric amplifier (OPA) system tuned to the CO_2 absorption peak and SPM in the buried GLS waveguide generates the spectrally broadened output centered on the absorption peak but reshaped to redistribute the spectrum to either side of the CO_2 absorption. The broadening occurs through the generation of side bands that are a well characterized feature of SPM as illustrated schematically in Fig. 1(a). This offers a potential route to tailor source spectra for maximum power delivery through the atmosphere, which is of interest both for directed infrared countermeasures (DIRCM) and remote sensing. As a consequence of the high nonlinearity of our GLS waveguide, we demonstrate not only self-phase modulation but also SC generation in the buried waveguide.

To generate the required 4.26 μm wavelength the signal and idler outputs of the optical parametric amplifier (Spectra-Physics OPA-800) were combined in a difference frequency generation (DFG) $AgGaS_2$ crystal. The OPA was pumped by a regeneratively amplified Ti:Sapphire laser system and was operated with a pulse repetition rate of 1 kHz. With the DFG crystal module, this system has a tunable wavelength range of 1100–6500 nm. Since there is strong absorption at 4.26 μm in the atmosphere due to the presence of carbon dioxide it was necessary to encase the DFG and waveguide coupling optics in a positive pressure chamber. A continuous flow of oxygen-free nitrogen was pumped into the chamber in order to displace the atmospheric carbon dioxide. A schematic of the experimental set-up is shown in Fig. 1(d). The co-propagating signal and idler beams are directed through a 1 mm thick CaF_2 window before being focused into the $AgGaS_2$ difference frequency crystal. The residual signal and idler power is then blocked by a long-pass 3000 nm filter. The difference frequency output was collimated and passed through an MgF_2 half-wave plate and a BaF_2 wire grid polarizer allowing power and polarization control. The pulse width of the difference frequency pulse train was estimated to be 120 fs based upon the measured pulse width of the signal and idler output. Incident power measurements were made by a pyro-electric detector (Laser Probe Inc RkP-575) accessed by lowering a flip mirror, the beam then passed through a calcium fluoride window and onto the detector. Two 20 mm focal length calcium fluoride lenses were used to couple and then collect the light from the test waveguides. Both the calcium fluoride lenses were mounted on separate x, y, z translation stages (Elliot Scientific MDE122). The waveguide substrate was mounted on a four axis translation stage (Thorlabs MBT401). By changing the position of a second flip mirror, the waveguide output could either be directed onto a camera (FLIR SC7000) in order to record the guided mode profiles, or onto a monochromator (Zolix Omni λ-300) to record the output spectrum. The monochromator was used in conjunction with a PbSe detector (Thorlabs PDA20H) and a lock-in amplifier in order to measure the spectral power distribution.

Due to residual CO_2 absorption outside of the purged chamber and in the monochromator the spectra are still affected by atmospheric absorption. This can be seen by observing the DFG spectrum as recorded by the monochromator. This spectrum is shown in Fig. 2 together with the theoretical input spectrum in the absence of CO_2 absorption. However, with the chamber purged, the DFG signal is launched into the waveguide without any significant attenuation. The waveguide output spectrum was recorded with an incident pulse energy of 410 nJ. The actual launched energy can be estimated by considering the mode size mismatch between the 45 μm MFD of the waveguide and the 22 μm MFD of the diffraction limited beam waist for the 20 mm focal length coupling lens with an input beam diameter of 5 mm. This was found to have a loss of 2.1 dB. The Fresnel loss from the glass—air interface is significant as GLS has a relatively high refractive index, which at 4260 nm was estimated to be 2.36. This was based upon extrapolation using the Sellmeier equation and a fit to index measurements reported in the literature.[24] This resulted in a Fresnel loss of 0.78 dB and a total coupling loss of 2.88 dB. Using this loss

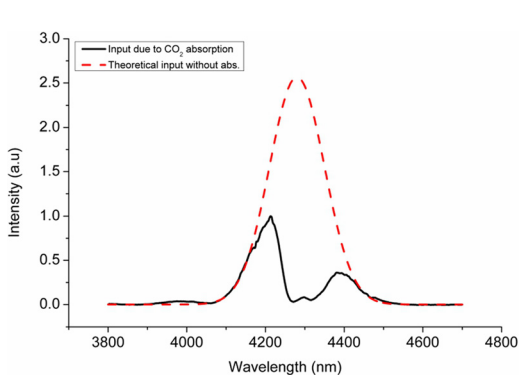

FIG. 2. Input pulse spectrum centred on 4260 nm that has been shaped by atmospheric CO_2 absorption (solid line). The fitted unmodified spectrum (broken line).

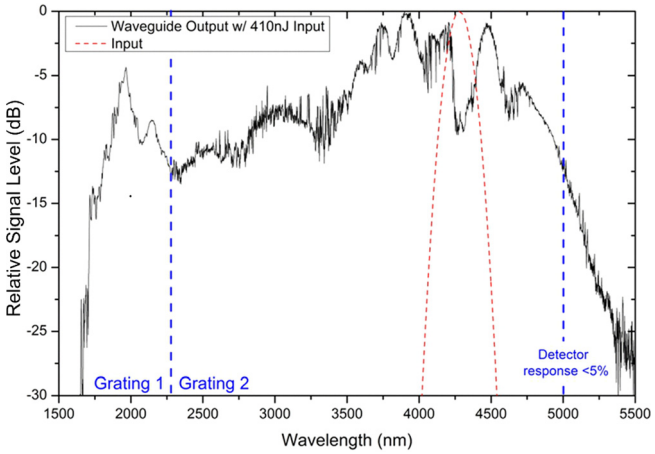

FIG. 3. Supercontinuum spectrum generated with a 410 nJ incident pulse energy, corresponding to an estimated coupled pulse energy of 211 nJ. The location and width of the input pulse spectrum is indicated by the broken red line at 4260 nm.

figure, the total coupled pulse energy was estimated to be 211 nJ and corresponds to a peak power of 1.76 MW.

The resulting spectral broadening can be seen in Fig. 3. It is clear from the incident pulse energy measurements that when the chamber is purged; the attenuation of the pump pulse is reduced greatly, enabling enough pulse energy to be coupled into the waveguide to generate nonlinear spectral broadening. This broadening can be seen to extend from 1750 nm to beyond 5000 nm at the −15 dB level and there is evidence of the super continuum extending to beyond 5500 nm, however, the detector responsivity in the current experimental setup is less than 5% beyond 5000 nm. This is the longest pump wavelength at which spectral broadening has been observed in a buried optical waveguide and spans the entire 3–5 μm atmospheric transmission window. Also, in contrast to earlier work where significant mid infrared continua were observed in bulk chalcogenide glass at peak power levels ranging from 3 to 20 MW,[9] the coupled pulse energy resulting in a similar super continuum width in our work is markedly smaller (1.76 MW), highlighting the benefit of a guided mode structure for efficient nonlinear spectral broadening. The high transmission of the GLS substrate used as our buried waveguide material extends to beyond 10 μm and thus is a promising platform for generating supercontinua that cover a large fraction of the chemical fingerprint region. The results presented demonstrate how high confinement geometries such as fiber tapers or nanowires are not required to demonstrate octave spanning mid infrared continuum. Larger mode area buried waveguide devices like those presented in this work can be more robust and more readily integrated with appropriate modular and compact optical pump sources compared to nanostructured devices such as fiber tapers and nano-wires. The development of guided mode devices in the mid infrared is of great importance for the future development of mid infrared photonic devices. Finally, we have demonstrated that centering the pump wavelength on the atmospheric CO_2 absorption peak can enable nonlinear spectral broadening to reshape the source spectrum and thereby enhance the transmission through the 3–5 μm atmospheric window. This will be of importance for the subsequent development of broadband sources for remote sensing and infrared countermeasures applications.

This work was funded by EPSRC and Selex ES through its Applied Research (EO) Programme in collaboration with the Stanford University, Scottish Universities Partnership (SU2P). H Bookey gratefully acknowledges support through a Royal Society of Edinburgh/Scottish Government Research Fellowship.

[1]P. Lucas, M. A. Solis, D. Le Coq, C. Juncker, M. R. Riley, J. Collier, D. E. Boesewetter, C. Boussard-Plédel, and B. Bureau, Sens. Actuators B **119**, 355–362 (2006).
[2]K. Ke, C. Xia, M. N. Islam, M. J. Welsh, and M. J. Freeman, Opt. Express **17**, 12627–12640 (2009).
[3]D. H. Titterton, Proc. SPIE **6451**, 64511Q (2007).
[4]A. Kosterev, G. Wysocki, Y. Bakhirkin, S. So, R. Lewicki, M. Fraser, F. Tittel, and R. F. Curl, Appl. Phys. B **90**, 165–176 (2008).
[5]K. E. Whittaker, L. Ciaffoni, G. Hancock, R. Peverall, and G. A. D. Ritchie, Appl. Phys. B **109**(2), 333–343, (2012).
[6]J. M. Dudley, G. Genty, and S. Coen, Rev. Mod. Phys. **78**, 1135–1184, (2006).
[7]J. M. Dudley, *Supercontinuum Generation in Optical Fibers*, (Cambridge University Press, Cambridge, 2010).
[8]R. A. Lamb, Proc. SPIE **8543**, 85430K (2012).
[9]Y. Yu, T. Wang, P. Ma, R. Wang, Z. Yang, D-Y. Choi, S. Madden and B. Luther-Davies, Opt. Mat. Express **3**(8), 1075–1086, (2013).
[10]A. Zakery and S. R. Elliott, J. Non-Cryst. Solids **330**, 1–12 (2003).
[11]D. W. Hewak, R. C. Moore, T. Schweizer, J. Wang, B. Samson, W. S. Brocklesby, D. N. Payne, and E. J. Tarbox, Electron. Lett. **32**(4), 384–385, (1996).
[12]W. Gao, M. El Amraoui, M. Liao, H. Kawashima, Z. Duan, D. Deng, T. Cheng, T. Suzuki, Y. Messaddeq, and Y. Ohishi, Opt. Express **21**, 9573–9583 (2013).
[13]J. Swiderski, M. Michalska, and G. Maze, Opt. Express **21**, 7851–7857 (2013).
[14]R. Buczynski, H. Bookey, D. Pysz, R. Stepien, I. Kujawa, J. McCarthy, A.Waddie, A. Kar, and M. Taghizadeh, Laser Phys. Lett. **7**, 666–672, (2010).
[15]A. Marandi, C. W. Rudy, V. G. Plotnichenko, E. M. Dianov, K. L. Vodopyanov, and R. L. Byer, Opt. Express **20**, 24218–24225 (2012).
[16]N. Granzow, M. A. Schmidt, W. Chang, L. Wang, Q. Coulombier, J. Troles, P. Toupin, I. Hartl, K. F. Lee, M. E. Fermann, L. Wondraczek, and P. St. J. Russell, Opt. Express **21**, 10969–10977 (2013).
[17]F. Silva, D. R. Austin, A. Thai, M. Baudisch, M. Hemmer, D. Faccio, A. Couairon, and J. Biegert, Nat. Commun. **3**, 807 (2012).
[18]M. Frumar, B. Frumarova, P. Nemec, T. Wagner, J. Jedelsky, and M. Hrdlicka, J. Non-Cryst. Solids **352**, 544–561 (2006).
[19]Z. G. Lian, W. J. Pan, D. Furniss, T. M Benson, A. B. Seddon, T. Kohoutek, J. Orava, and T. Wagner, Opt. Lett. **34**, 1234–1236 (2009).
[20]N. D. Psaila, R. R. Thomson, H. T. Bookey, S. Shen, N. Chiodo, R. Osellame, G. Cerullo, A. Jha, and A. K. Kar, Opt. Express **15**, 15776–15781 (2007).
[21]J. E. McCarthy, H. T. Bookey, N. D. Psaila, R. R. Thomson, and A. K. Kar, Opt. Express **20**, 1545–1551 (2012).
[22]S. Nolte, M. Will, J. Burghoff, and A. Tuennermann, Appl. Phys. A. **77**, 109–111 (2003).
[23]Y. Nasu, M. Kohtoku, and Y. Hibino, Opt. Lett. **30**, 723–725 (2005).
[24]H. Yayama, S. Fujino, H. Takebe, K. Morinaga, and D. W. Hewak, J. Non-Cryst. Solids **239**, 187–191 (1998).